AAS 20-636

MODELING RE-ENTRY BREAK-UP UNCERTAINTIES WITH CONTINUITY EQUATION AND GAUSSIAN MIXTURE MODELS INTERPOLATION

Mirko Trisolini* **and Camilla Colombo†**

The effect of uncertainties in the re-entry and break-up of satellites is analyzed. Two contributions are considered: the effect of the initial uncertainties of the parent trajectory and the break-up event, characterized by high thermal and mechanical loads and tumbling motion. Specifically, this last phenomenon may cause the scattering of the components off the nominal trajectory of the parent spacecraft. The presented study describes the uncertainties and the break-up event through probability distributions, propagates them using a continuum approach, and reconstructs the uncertainties at future states using the Starling suite developed at Politecnico di Milano.

INTRODUCTION

The study and prediction of the re-entry and demise of spacecraft and rocket bodies is a challenging task. Several factors may influence the accuracy of these predictions, such as the knowledge of the initial entry conditions, the ballistic coefficient of the satellite, the modeling of the heat load affecting the S/C structure and components. The uncertainties associated with these parameters can have a substantial effect on the evolution of the re-entry trajectory and on the risk the surviving objects may pose to people and properties on the ground. In the past sixty years, an average of 93 uncontrolled re-entries per year[1] have been documented. With the increasing of the space activity, the number of objects in orbit is destined to grow rapidly and, with it, the frequency of re-entries. This underlines the importance of statistically based re-entry simulations for better studying of the demisability of re-entering objects. Indeed, considering the effects of uncertainties, it is possible to assess the demise probability of specific components,[2] the statistical distribution and the casualty area of each surviving object, and combining it with the landing footprint and the population distribution.

The standard procedure for the assessment of uncertainties is through a Monte Carlo based dispersion analysis. With this approach, a large number of simulations over randomly sampled states allow the estimation of the joint Probability Density Function (PDF) through a frequentist approach. As the quality of the results of Monte Carlo (MC) simulations is strongly affected by the number of samples, a reliable uncertainty analysis can only be obtained through computationally expensive simulations, especially for high-dimensional and non-linear dynamics such as the ones associated with re-entry scenarios.

*PostDoctoral Researcher, Dipartimento di scienze e tecnologie aerospaziali, Politecnico di Milano, via La Masa 34, 10156, Milano.

†Associate Professor, Dipartimento di scienze e tecnologie aerospaziali, Politecnico di Milano, via La Masa 34, 10156, Milano.

The present study, instead, proposes a methodology for the propagation and assessment of uncertainties based on a continuum approach.[3–5] With this method, the continuity equation is coupled with the re-entry dynamics to obtain the actual value of the probability density as it evolves over time through the characteristics of the system. Such a methodology directly compares to Monte Carlo simulations: while with MC methods we propagate individual realization of the initial PDF, with a continuum-based approach we propagate the ensemble of realizations conserving the total probability mass in the state space throughout the simulation. As each sample of the continuum-based methodology carries the true value of the probability density, this methodology allows for a lower number of simulations with respect to the MC method. However, the value of the density is only known at discrete points in the state space. Therefore, a reconstruction methodology must be used to obtain the uncertainty distribution in the entire domain. In this work, a fitting is performed using the Starling suite developed at the Politecnico di Milano, which is based on Gaussian Mixture Models (GMM).[7]

The break-up process is highly erratic and is usually characterized by high accelerations and a tumbling motion. This introduces another source of uncertainty as the internal components can be scattered by this process, thus deviating from the nominal trajectory of the parent spacecraft. In this work, we consider this uncertainty by adapting the NASA Standard Break-up Model (SBM)[8] to generate a distribution of Δv impulses that are imparted to the internal components at the moment of the break-up. This is considered on top of the uncertainty that are intrinsic to the parent spacecraft at the break-up condition. Combining these contributions, a statistically meaningful picture of the the re-entry event can be obtained. this is especially true when this approach is used with object-oriented codes,[9–13,19] which rely on a simplified description of the dynamics and aerothermodynamics.

The first part of this work is dedicated to the application and adaptation of the continuum-based approach to the re-entry problem, the second part is dedicated to the modeling of the break-up event through the NASA SBM, while the last part shows an application of the methodology to a representative test case and how the methodology can be used to compute the casualty risk on ground.

METHODOLOGY

This section describes the dynamical model used to propagate the uncertainty distribution, which is based on the continuity equation, and the model used to describe the uncertainties at the break-up event. The final part will briefly describe the use of the GMM-based fitting methodology of the Starling suite[7] to reconstruct the uncertainty distribution.

Continuum-based propagation

The proposed methodology is based on the continuum approach for the propagation of the probability density of re-entry uncertainties. This can be obtained applying the continuity equation to the specific dynamical problem in exam.

$$\frac{\partial n(\mathbf{x},t)}{\partial t} + \nabla \cdot \mathbf{f}(\mathbf{x}) = \dot{n}^{+} - \dot{n}^{-}, \tag{1}$$

where $n(\mathbf{x},t)$ is the density at time t and state $\mathbf{x}$, $\nabla \cdot \mathbf{f}(\mathbf{x})$ represents the forces acting on the system from slow, continuous phenomena such as gravity and atmospheric drag, and $\dot{n}^{+} - \dot{n}^{-}$ represents the fast and discontinuous events (sources and sinks). For the case in exam, the source and sink terms

are neglected. Knowing the probability density distribution at the initial time, $n(\mathbf{x}, 0)$, Equation (1) allows the propagation of the density evolution in time. This is a Partial Differential Equation (PDE) with the joint Probability Distribution Function (PDF) $n(\mathbf{x}, t)$ being the dependent variable. Such an equation regulates the conservation of the total probability mass of the joint PDF through its spatial-temporal evolution due to the forces acting on the system.

Equation (1) can be solved using the Method of Characteristics (MOC), where the partial differential equation is transformed into a set of Ordinary Differential Equations (ODE) as follows:[3]

$$\begin{cases} \frac{\mathrm{d}\alpha_1}{\mathrm{d}s} = v_{\alpha_1}(\alpha_1, \ldots, \alpha_m) \\ \ldots \\ \frac{\mathrm{d}\alpha_m}{\mathrm{d}s} = v_{\alpha_m}(\alpha_1, \ldots, \alpha_m) \\ \frac{\mathrm{d}n}{\mathrm{d}s} = -\left[\frac{\partial v_{\alpha_1}}{\partial \alpha_1} + \cdots + \frac{\partial v_{\alpha_m}}{\partial \alpha_m}\right] \cdot n(\alpha_1, \ldots, \alpha_m) \end{cases}, \tag{2}$$

where s is the independent variable, $(\alpha_1, \ldots, \alpha_m)$ are the state variables of the system. It is possible to observe how the evolution of the density is regulated by the trace of the Jacobian of the dynamics describing the system. As it is convenient to express the evolution of the re-entry trajectory using re-entry parameters, we specialize Equation (2) to the re-entry problem, where we have used the radius as the independent variable.

$$\begin{cases} \frac{\mathrm{d}\lambda}{\mathrm{d}r} = \frac{\sin(\chi)}{r\cos(\varphi)\tan(\gamma)} \\ \frac{\mathrm{d}\varphi}{\mathrm{d}r} = \frac{\cos(\chi)}{r\tan(\gamma)} \\ \frac{\mathrm{d}v}{\mathrm{d}r} = -\frac{v\rho(r)}{2\beta\sin(\gamma)} - \frac{1}{v}\left(g_r(r,\varphi) + \frac{\cos(\chi)g_\varphi(r,\varphi)}{\tan(\gamma)}\right) + \frac{r\omega_p^2\cos(\varphi)}{v}\left(\cos(\varphi) - \frac{\cos(\chi)\sin(\varphi)}{\tan(\gamma)}\right) \\ \frac{\mathrm{d}\gamma}{\mathrm{d}r} = \frac{\alpha\rho(r)}{2\sin(\gamma)} - \frac{1}{v^2\tan(\gamma)}\left(g_r(r,\varphi) + \cos(\chi)\tan(\gamma)g_\varphi(r,\varphi) - \frac{v^2}{r}\right) + \frac{2\omega\sin(\chi)\cos(\varphi)}{v\sin(\gamma)} + \\ \qquad + \frac{r\omega_p^2\cos(\varphi)}{v}\left(\frac{\cos(\varphi)}{\tan(\gamma)} + \cos(\chi)\sin(\varphi)\right) \\ \frac{\mathrm{d}\chi}{\mathrm{d}r} = \frac{\sin(\chi)\tan(\varphi)}{r\tan(\gamma)} + \frac{2\omega_p}{v}\left(\frac{\sin(\varphi)}{\sin(\gamma)} - \frac{\cos(\chi)\cos(\varphi)}{\cos(\gamma)}\right) + \\ \qquad + \frac{\sin(\chi)}{v^2\sin(\gamma)\cos(\gamma)}\left(r\omega_p^2\sin(\varphi)\cos(\varphi) - g_\varphi(r,\varphi)\right) \\ \frac{\mathrm{d}\beta}{\mathrm{d}r} = 0 \\ \frac{\mathrm{d}n}{\mathrm{d}r} = -\left[\frac{\partial\lambda'}{\partial\lambda} + \frac{\partial\varphi'}{\partial\varphi} + \frac{\partial v'}{\partial v} + \frac{\partial\gamma'}{\partial\gamma} + \frac{\partial\chi'}{\partial\chi} + \frac{\partial\beta'}{\partial\beta}\right]n \end{cases} \tag{3}$$

where λ is the longitude, φ the latitude, v the velocity, γ the flight-path angle, $\beta = \frac{m}{C_D S}$ the ballistic coefficient, $\alpha = \frac{C_L S}{m}$ a modified lift coefficient of the re-entering object, and g_r and g_φ are the radial and transversal components of the gravitational acceleration, respectively. The expression for the derivative of the density as a function of r has not been expanded for a better readability. In this expression, the primes refers to partial derivatives with respect to the radius. Any gravitational and atmospheric model can be used, as long as they can be modeled with a continuous and differentiable function. For the case in exam, the 1976 US Standard Atmosphere[14] was considered for the atmosphere and a model including the effects of J_2 for the gravitational acceleration.[15]

The system of Equation (3) has to be numerically integrated. The integration can be performed using a standard ODE solver such as the Runge-Kutta method. In such fashion, the time evolution of the density in the considered state space can be obtained for a specified set of time instants. As the solution for the re-entry problem is not analytical, it is necessary to sample the initial density distribution and to integrate the system of Equation (3) for each one of the sampled points. Subsequently, the distribution can be reconstructed at each time step by fitting the scattered data over the state space domain.

Break-up uncertainties

As previously introduced, the motion of the parent spacecraft as it approaches the break-up can become erratic. This can influence the state of the internal components as they are released when the external structure starts to shed. We decided to take into account this contribution as an uncertainty in the release velocity and direction of the internal components. To do so, we borrowed the NASA Standard Break-up Model (SBM)[8] and modelled the ejection velocity of a component at break-up through a log-normal distribution as follows:

$$p_{\Delta v}(\chi, \nu) = \mathcal{N}(\mu(\chi), \sigma(\chi), \nu), \tag{4}$$

where $\mathcal{N}$ is a Normal distribution, $\chi = \log_{10}(A/M)$ is the logarithm in base ten of the area-to-mass ratio, $\nu = \log_{10}(\Delta v)$, and $\mu(\chi) = 1.85 + 0.2 \cdot \chi$ and $\sigma(\chi) = 0.4$ are the mean and standard deviation of the Normal distribution. In the NASA SBM these values depend on the type of event, whether an explosion or a collision is considered. For the case in exam, we considered an explosion, assuming that the break-up can be more closely described by such an event. In general, the NASA SBM also provides the distribution of the fragments area-to-mass ratio. This feature can be used in two different ways: considering also a fragmentation of the component and modeling the distribution of the generated fragment, or considering an uncertainty in the area-to-mass ratio of the component analyzed (e.g. a not precisely known cross-section or mass of the object), which in results in a different ejection velocity being imparted to the component.

The NASA SBM was chosen as it has already been adopted in ESA DRAMA to describe the possible explosions and consequent fragmentation of components during re-entry.[16] In that context it was used by directly sampling the distribution to generate the fragments in a Monte Carlo fashion. In this case, it is used to model the ejection velocity and direction that can be imparted to a component during the break-up event. The distribution obtained with the NASA SBM is used, also in combination with the parent spacecraft uncertainties, to obtain a fully statistical description of the event. However, this is only a preliminary application to showcase the possibility to include such uncertainties in the re-entry process. Any type of fragmentation model that can be represented with distributions can be included in the presented methodology.

Equation (4) provides the expression for probability distribution of Δv as a function of ν. The first step is thus to transform it into an expression as a function of Δv as follows:

$$p_{A/M,\Delta v}(A/M, \Delta v) = \frac{p_{\Delta v}(\chi, \nu)}{\log(10)^2 \cdot \Delta v \cdot A/M}. \tag{5}$$

where $p_{\Delta v}(\chi, \nu)$ is the distribution obtained from the NASA SBM in the variables χ and ν, $Deltav$ is the impulse imparted to the object, and A/M is the area-to-mass ratio of the object.

The probability value $p_{\Delta v}(\Delta v)$ can be then obtained by marginalization of Equation (5). In case the value of the area-to-mass ratio, A/M, is constant, the probability for the velocity impulse can be readily obtained without marginalization. The Δv provided by the NASA SBM only gives the absolute value of the impulse; however, to properly model the break-up we consider that the ejection can happen randomly in any direction relative to the S/C re-entry velocity. Therefore, the provided impulse is transformed into a vector quantity $\Delta\mathbf{v} = (\Delta v_x, \Delta v_y, \Delta v_z)$, where the x axis is oriented along the North direction, the z axis is oriented along the radial direction, ant the y axis comes from applying the right-hand rule (Figure 1).

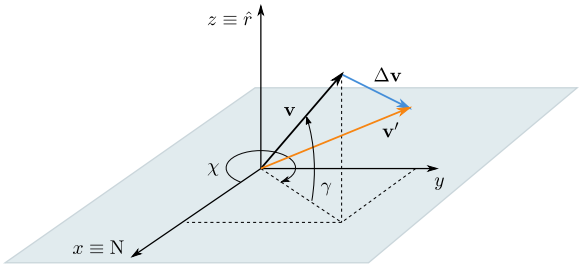

Figure 1: Reference frame for the velocity decomposition to compute the velocity after the break-up impulse.

The decomposition of the absolute velocity into its components, requires a transformation of the probability density of Equation (4) as follows:

$$p_{\Delta\mathbf{v}}(\Delta\mathbf{v}) = \frac{p_{\Delta v}(\Delta v)}{4\pi\Delta v^2}, \tag{6}$$

where this expression is valid for a two-dimensional case like the one considered by the dynamical model of Equation (3). The contribution of the $\Delta\mathbf{v}$ impulse is then summed to the velocity of the object before the break-up event. In this work, this is assumed to be equal to the velocity of the parent spacecraft at break-up. Therefore, after the impulse is given, the component will have modified values of the velocity magnitude, flight-path angle, and heading angle according to the following transformation:

$$\varphi : \begin{cases} \hat{v} = \sqrt{(v_x + \Delta v_x)^2 + (v_y + \Delta v_y)^2 + (v_z + \Delta v_z)^2} & (7) \\ \hat{\gamma} = \arctan\left(\dfrac{v_z + \Delta v_z}{\sqrt{(v_x + \Delta v_x)^2 + (v_y + \Delta v_y)^2}}\right) & (8) \\ \hat{\chi} = \arctan\left(\dfrac{v_y + \Delta v_y}{v_x + \Delta v_x}\right) & (9) \end{cases}$$

where $\hat{v}$, $\hat{\gamma}$, and $\hat{\chi}$ are the velocity magnitude, flight-path angle, and heading angle after the break-up, and v_x, v_y, and v_z are the same components before the break-up, expressed in the same reference frame as the Δv components, which can be expressed as follows:

$$\begin{cases} v_x = v\cos\gamma\cos(2\pi - \chi) \\ v_y = v\cos\gamma\sin(2\pi - \chi) \\ v_z = v\sin\gamma \end{cases} \tag{10}$$

If a single value of the velocity, flight-path angle, and heading angle before the breakup is provided, the new distribution follows the shape of Equation (6). An example of such a distribution is provided in Figure 2, where the *nominal* values are set as 7.2 $\mathrm{km\,s^{-1}}$ for the velocity, -2.5° for the flight-path angle, and 10° for the heading angle.

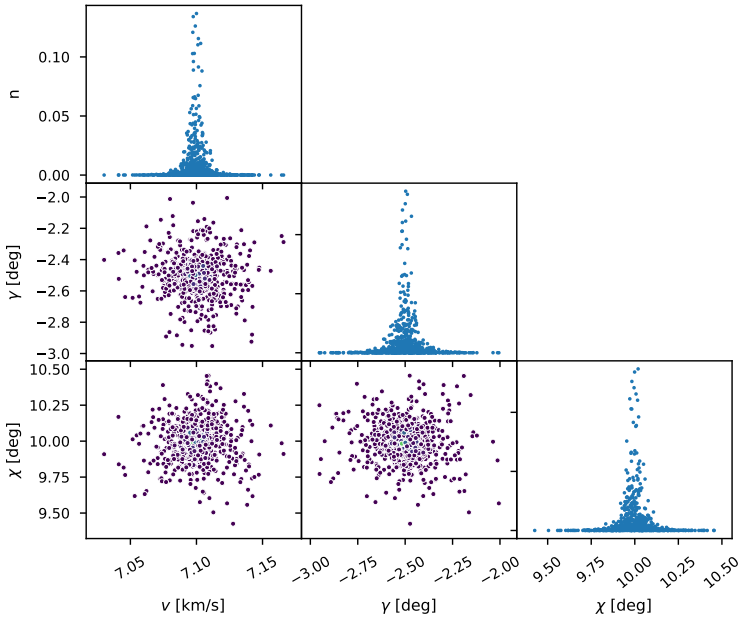

Figure 2: Example of samples obtained after the break-up by summing the NASA SB distribution to a set of initial conditions.

Figure 2 shows the projection of the samples along the (v, γ, χ) direction and on the diagonal the magnitude of the probability density for each sample. It is possible to observe how the probability is mostly concentrated around the nominal values as the Δv provided by the NASA SBM have, on average, a small values. However, the obtained distribution has a range of about 0.1 $\mathrm{km\,s^{-1}}$ for the velocity and 1° for the flight-path angle and heading angle.

However, the distribution of the break-up impulse can also be overlapped to the uncertainty at break-up of the parent spacecraft. For example, considering the parent spacecraft at break-up point has an uncertainty $p(v, \gamma, \chi)$, and assuming the impulse uncertainty $p_{\Delta\mathbf{v}}(\Delta\mathbf{v})$ is independent from this state, we can create an extended probability distribution as follows:

$$p(v, \gamma, \chi, \Delta v_x, \Delta v_y, \Delta v_z) = p(v, \gamma, \chi) \cdot p(\Delta v_x, \Delta v_y, \Delta v_z). \tag{11}$$

Once we have this distribution, we can apply the transformation of Equation (7) and using the Dirac generalized transformation we can obtain the distribution in the new variables after the break-up $(\hat{v}, \hat{\gamma}, \hat{\chi})$.

$$p(\hat{v},\hat{\gamma},\hat{\chi}) = \int p(v_x,v_y,v_z,\Delta\mathbf{v})\ \delta(\hat{v}-\varphi_1)\ \delta(\hat{\gamma}-\varphi_2)\delta(\hat{\chi}-\varphi_3)\ dv_x\, dv_y dv_z\, d\Delta\mathbf{v}$$
$$= \iiint \frac{p(\hat{v},\hat{\gamma},\hat{\chi},\Delta\mathbf{v})}{|\det J(\varphi)|}\ d\Delta v_x\, d\Delta v_y\, d\Delta v_z, \tag{12}$$

where $\det J(\varphi)$ is the determinant of the Jacobian of the φ transformation (Equation (7)).

$$\det J(\varphi) = \begin{vmatrix} \frac{\partial\varphi_1}{\partial v_x} & \frac{\partial\varphi_1}{\partial v_y} & \frac{\partial\varphi_1}{\partial v_z} \\ \frac{\partial\varphi_2}{\partial v_x} & \frac{\partial\varphi_2}{\partial v_y} & \frac{\partial\varphi_2}{\partial v_z} \\ \frac{\partial\varphi_3}{\partial v_x} & \frac{\partial\varphi_3}{\partial v_y} & \frac{\partial\varphi_3}{\partial v_z} \end{vmatrix}$$
$$= -\frac{\left((v_x+\Delta v_x)^2+(v_y+\Delta v_y)^2+(v_z+\Delta v_z)^2\right)^{-\frac{1}{2}}}{\sqrt{(v_x+\Delta v_x)^2+(v_y+\Delta v_y)^2}} \tag{13}$$

The values of v_x, v_y, and v_z are then obtained inverting the transformation φ. It has to be noted here that the transformation has been performed starting from the velocity components before the break-up in the (x, y, z) frame. This requires a first transformation using Equation (10), which also modifies the probability density as follows:

$$p(v_x,v_y,v_z) = \frac{p(v,\gamma,\chi)}{v^2\cos\gamma}, \tag{14}$$

where the denominator is the Jacobian of the transformation Equation (10).

RESULTS

The methodology presented in Methodology is applied to a representative test case. The trajectory of a *parent* space if first simulated from an altitude of 100 km up to a specified break-up altitude. In this case, we consider a standard break-up altitude of 78 km. The characteristics of the *parent* spacecraft, the initial conditions, and the uncertainty associated to them are summarized in Table 1. The re-entry conditions are representative of a uncontrolled shallow entry.

The trajectory of the parent spacecraft is then simulated using Equation (3) up to the break-up altitude. Here the scattered samples, which also carry the density information, allow the reconstruction of the probability density at the considered snapshot. To perform such a reconstruction we use the Starling suite[7] developed at the Politecnico di Milano, which is based on Gaussian Mixture Models. The obtained distribution in (λ, φ, v, γ, χ) is then combined with the distribution of the break-up impulse obtained from the NASA SBM through Equation (7) and Equation (12) to obtain the initial conditions of the re-entry of the internal components released from the *parent* spacecraft. To obtain the distribution it is also necessary to provide the area-to-mass ratio of the considered component (to be used inside the NASA SBM). For this test case, we selected as sample component a reaction wheel, which is one of the components that usually survive re-entry as they are produced with high melting point materials. The characteristics of the considered reaction wheel are summarized in Table 2.

Table 1: Mean and standard deviation for the initial conditions of the parent spacecraft and values of the relevant parameters.

State	Symbol	Unit	μ	σ
Initial longitude	λ_0	$^\circ$	10.0	0.2
Initial latitude	φ_0	$^\circ$	0.0	0.2
Initial velocity	v_0	$\mathrm{km/s}$	7.6	0.012
Initial flight-path angle	γ_0	$^\circ$	-1.5	0.05
Initial heading angle	χ_0	$^\circ$	90	0.2
Parameter	Symbol	Unit	Value	
Initial altitude	h_0	km	100	
Ballistic coefficient	β	$\mathrm{kg/m^2}$	500.0	
Lift coefficient	α	$\mathrm{m^2/kg}$	0.0	

Table 2: Characteristics of the reaction wheel used in the test case.[17]

State	Symbol	Unit	Value
Diameter	D	cm	15.66
Height	H	cm	6.26
Mass	m	kg	7.45
Drag coefficient	C_D		1.535
Cross-section (average)	S	$\mathrm{m^2}$	0.0161
Ballistic coefficient	β	$\mathrm{kg\,m^{-2}}$	301.5
Lift coefficient	α	$\mathrm{m^2/kg}$	0

The drag coefficient considers only the hypersonic regime[13,18,19] and is assumed to be constant for the entire re-entry. In this test case, we consider only the ejection contribution imparted to the component at break-up while it remains intact and does no fragment. This is typical for heavy metallic objects such as reaction wheels and tanks. Figure 3 shows the initial conditions for the reaction wheel after the break-up at an altitude of 78 km.

The samples of Figure 3 are then propagated using Equation (3) until landing. The resulting snapshot is the one presented in Figure 4. It is visible the deformation of the state space, particularly in the v-γ plane. Overlapping the sampled points, it is possible to observe the results of the fitting using the Starling suite. In the off-diagonal plots, the orange crosses represent the location of the kernels of the GMM regression, while in the diagonal plots the marginal probability for each variable is shown. The orange line is the marginal obtained by integrating the GMM and in cyan the corresponding histogram obtained in a Monte Carlo fashion.

Once the fitting of the landing snapshot is obtained, we can isolate the two-dimensional marginal distribution of interest, which is the one in longitude and latitude. In this way, we obtain the probability distribution of the landing location of the considered component (Figure 5a), which can be used to compute the casualty risk associated to the component landing at the predicted location.

Casualty risk computation

In general, the casualty risk, E_c, is computed as:

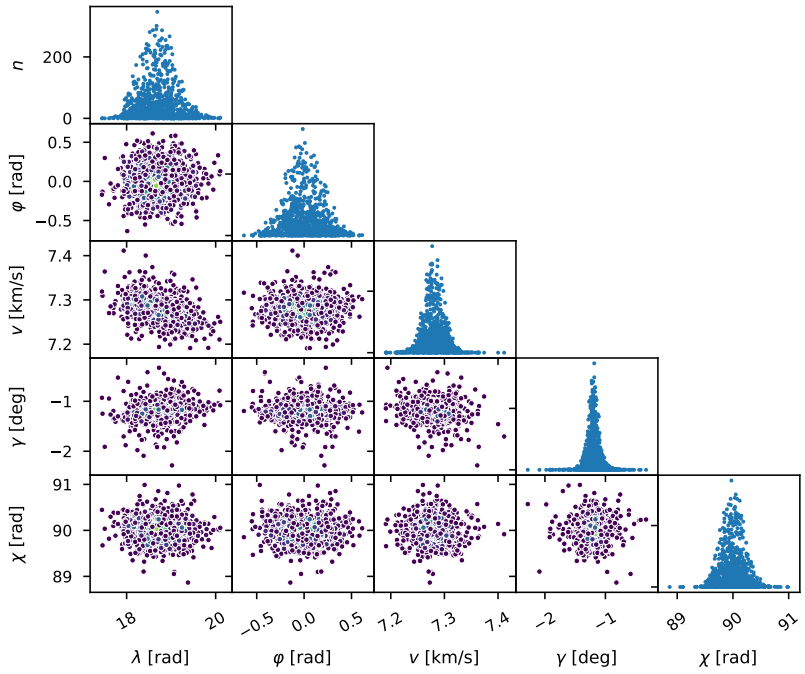

Figure 3: Initial conditions for the re-entry of the reaction wheel.

$$E_{\mathrm{C}} = A_{\mathrm{C}} \cdot \frac{N_p}{S_p}, \tag{15}$$

where N_p is the population count for the considered landing location, S_p is the corresponding surface area of the landing location, and $A_C = (\sqrt{A_{\mathrm{obj}}} + \sqrt{A_{\mathrm{h}}})^2$ is the casualty area. The term A_{obj} is the average cross-section of the landed component and $A_{\mathrm{h}} = 0.36\ \mathrm{m}^2$ is the average cross-section of a person. This expression can be modified to include the probability information we can obtain from integrating and fitting the probability density in longitude and latitude as follows:

$$E_{\mathrm{C}} = \sum_{i=1}^{N_g} A_{\mathrm{C}} \cdot p_i \cdot \frac{N_{p,i}}{S_{p,i}}, \tag{16}$$

where N_g is the number of grid subdivisions used in discretizing the longitude-latitude area covered by the predicted landing location, $N_{p,i}$ and $S_{p,i}$ are the population count and surface area relative to the i-th grid subdivision respectively, p_i is the probability of the object landing in the area identified by the i-th grid subdivision, and A_{C} is considered constant in this example. Equation (16) is equivalent to a weighted sum of the casualty risk value for each grid cell in which the landing location is subdivided, with the weight being the predicted impact probability.

To compute the casualty risk for the presented example of the re-entry of a reaction wheel, we have used the UN-WPP Adjusted Population Data[20] with a resolution of 0.25°. Figure 5b shows the resulting population density for the landing location. Combining the impact probability of Figure 5a

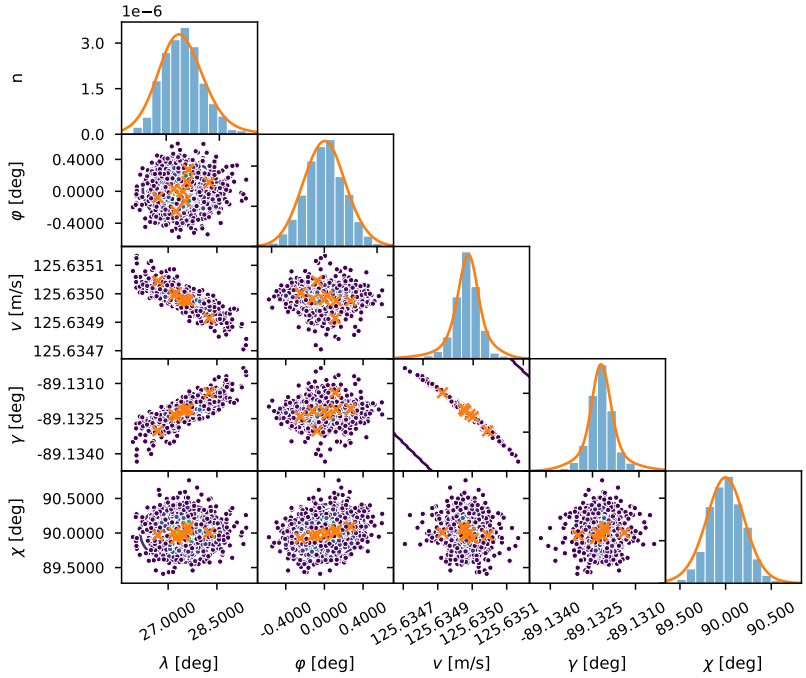

Figure 4: Snapshot fit of the landing conditions for the re-entry of the reaction wheel using the Starling suite. The off-diagonal elements represent the projections of the scattered points. The orange crosses are the locations of the kernels of the GMM fit obtained with Starling. The diagonal plots represent instead the marginal plots: in blue the histogram obtained from the scattered points and in orange the marginals obtained with Starling.

with the population density we obtain the risk map (in log scale) of Figure 5c, which corresponds to the risk per unit area for the considered grid in longitude and latitude. Finally, using this map with a constant cross-section for the reaction wheel ($A_{\text{obj}} = 0.0161$ m^2) and applying Equation (16) we obtain a value of the casualty risk of $E_{\text{C}} = 1.1 \times 10^{-5}$.

CONCLUSIONS AND FUTURE WORK

The work presented in this contribution has outlined a methodology to propagate and reconstruct re-entry uncertainties using the continuity equation and Gaussian Mixture Models. In addition, using the same tools combined with the NASA Standard Break-up Model, the introduction of uncertainties due to the break-up of the *parent* spacecraft on the release of internal components have been taken into account in the re-entry process. The models were applied to a representative test case in which a spacecraft trajectory is propagated until break-up and its uncertainties are then used in combination with a break-up model to obtain the initial conditions for the release of an internal component. In this particular case, the re-entry of a reaction wheel has been considered. The results show that the continuum propagation combined with the Starling suite is able to capture the evolution of the trajectory and its uncertainties with a limited number of samples. In addition, the marginal distribution in longitude and latitude can be readily obtained and used for the prediction of the on-ground casualty risk. This is achieved by combining the resulting landing probability

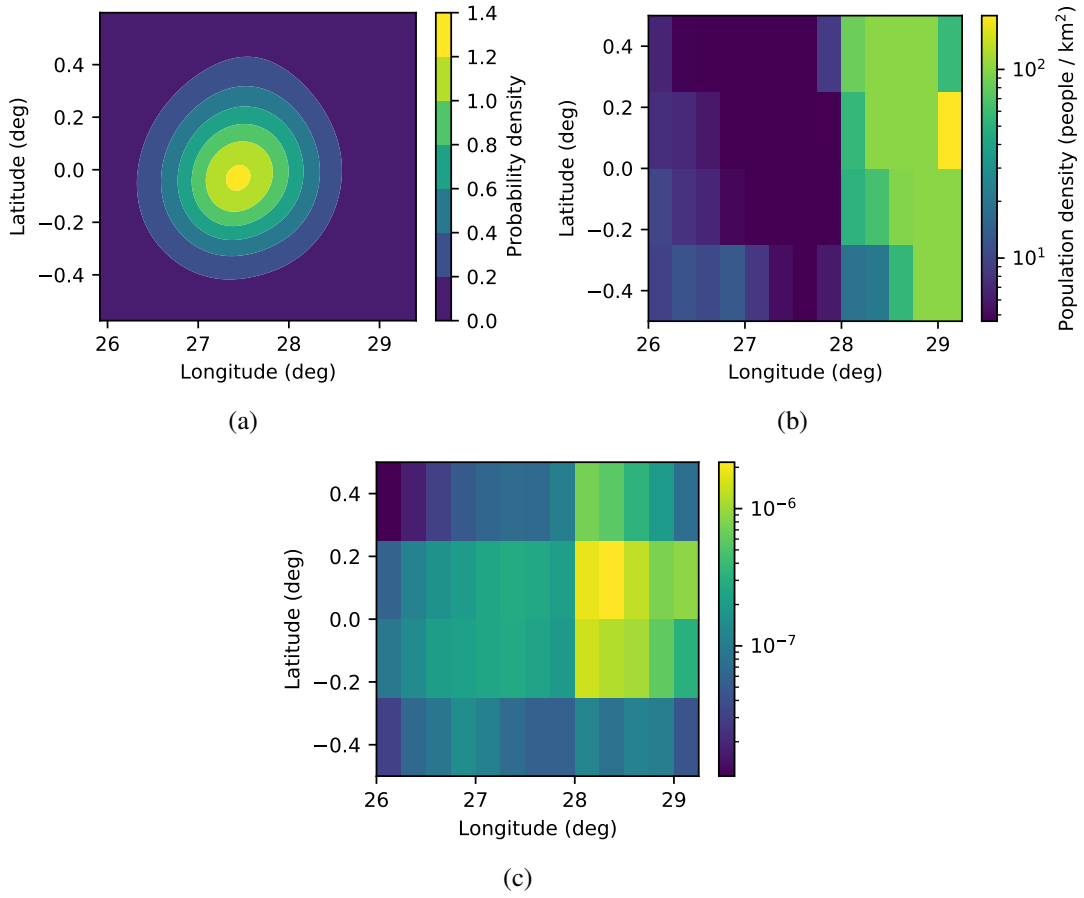

Figure 5: Landing probability map in longitude and latitude (a), Population density at the landing location (b), and risk map obtained combining the population density with the landing probability (c).

with the population density in the same area and the casualty area of the surviving fragment, giving a more realistic and statistically sound prediction. The proposed model has been applied to a standard test case and several features can still be improved for a better prediction of the casualty expectation. For example, more realistic atmospheric models may be used, which also account for uncertainties in the atmospheric quantities, uncertainty in the break-up altitude can be included as it is a difficult parameter to predict in advance, and the demise of the components can be accounted for. Nonetheless, the presented methodology can be further improved to include these features and future work will focus on these developments. In addition, the break-up event has been modeled borrowing the results of the NASA SBM, which has been specifically developed for orbital fragmentation, and therefore has a limited validity in the re-entry realm, despite it has already been used in such a context. However, the architecture of the methodology is very general and only requires a break-up model that is able to to return the distribution of the velocity impulses imparted to the internal components at the release moment. If more realistic break-up models will be available in the future, they can be readily implemented in the presented methodology.

FUNDING SOURCES

This project has received funding from the European Research Council (ERC) under the European Union's Horizon 2020 research and innovation programme (grant agreement No 679086 - COMPASS).

REFERENCES

[1] C. Pardini and L. Anselmo, "Re-entry predictions for uncontrolled satellites: results and challenges," *6th International Association for Space Safety Conference*, Montreal, Canada, 2013.

[2] M. Trisolini, H. G. Lewis, and C. Colombo, "Demisability and survivability sensitivity to design-for-demise techniques," *Acta Astronautica*, Vol. 145, 2018, pp. 357–384, 10.1016/j.actaastro.2018.01.050.

[3] N. N. Gor'kavyi, L. M. Ozernoy, and J. C. Mather, "A New Approach to Dynamical Evolution of Interplanetary Dust," *The Astrophysical Journal*, Vol. 474, jan 1997, pp. 496–502, 10.1086/303440.

[4] C. R. McInnes, "Autonomous ring formation for a planar constellation of satellites," *Journal of Guidance, Control, and Dynamics*, Vol. 18, No. 5, 1995, pp. 1215–1217, 10.2514/3.21531.

[5] M. Trisolini and C. Colombo, "A density-based approach to the propagation of re-entry uncertainties," *29th AAS/AIAA Space Flight Mechanics Meeting*, Ka'anapali, Hawaii, USA, 2019, pp. 1–13.

[6] M. Trisolini and C. Colombo, "A density-based approach to the propagation of re-entry uncertainties," *27th International Symposium on Space Flight Dynamics*, Melbourne, Australia, 2019.

[7] S. Frey, C. Colombo, S. Lemmens, *et al.*, "Application of density-based propagation to fragment clouds using the Starling suite," *1st International Orbital Debris Conference (IOC)*, 2019, pp. 1–10.

[8] N. L. Johnson, P. Krisko, J.-C. Liou, and P. Anz-Meador, "NASA's new breakup model of EVOLVE 4.0," *Advances in Space Research*, Vol. 28, No. 9, 2001, pp. 1377–1384.

[9] J. Dobarco-Otero, R. Smith, K. Bledsoe, R. Delaune, W. Rochelle, and N. Johnson, "The Object Reentry Survival Analysis Tool (ORSAT)-version 6.0 and its application to spacecraft entry," *Proceedings of the 56th Congress of the International Astronautical Federation, the International Academy of Astronautics, and International Institute of Space Law, IAC-05-B6*, Vol. 3, 2005, pp. 17–21.

[10] J. Gelhaus, N. Sanchez-Ortiz, V. Braun, C. Kebschull, J. C. d. Oliveira, R. Dominguez-Gonzalez, C. Wiedemann, H. Krag, and P. Vorsmann, "Upgrade of DRAMA-ESA's Space Debris Mitigation Analysis Tool Suite," *ESA Special Publication*, Vol. 723, 2013, p. 62.

[11] M. Trisolini, H. G. Lewis, and C. Colombo, "Survivability and Demise Criteria for Sustainable Spacecraft Design," *66th International Astronautical Conference*, Jerusalem, 2015.

[12] M. Trisolini, H. G. Lewis, and C. Colombo, "Demisability and survivability multi-objective optimisation for preliminary spacecraft design," *68th International Astronautical Congress*, Adelaide, Australia, 2017.

[13] M. Trisolini, H. G. Lewis, and C. Colombo, "Demise and Survivability Criteria for Spacecraft Design Optimization," *Journal of Space Safety Engineering*, Vol. 3, No. 2, 2016, pp. 83–93, 10.1016/S2468-8967(16)30023-4.

[14] National Oceanic and Atmospheric Administration, "U.S. Standard Atmosphere 1976," 1976.

[15] A. Tewari, *Atmospheric and Space Flight Dynamics: Modeling and Simulation with MATLAB® and Simulink®*. Birkhäuser, 2007.

[16] J. Gelhaus, C. Kebschull, V. Braun, N. Sanchez-Ortiz, E. Parilla Endrino, J. C. d. Oliveira, and R. Dominguez-Gonzalez, "Upgrade of ESA's Space Debris Mitigation Analysis Tool Suite," Tech. Rep. ESA contract 4000104977/11/D/SR, European Space Agency, 2014.

[17] Bradford Space, "Reaction Wheel Unit," https://www.bradford-space.com/products-aocs-reaction-wheel-unit.php. Accessed: 2020-07-10.

[18] R. D. Klett, "Drag Coefficients and Heating Ratios for Right Circular Cylinder in Free-Molecular and Continuum Flow from Mach 10 to 30," 1964, 10.2172/4630398.

[19] M. Trisolini, H. G. Lewis, and C. Colombo, "Spacecraft design optimisation for demise and survivability," *Aerospace Science and Technology*, Vol. 77, jun 2018, pp. 638–657, 10.1016/j.ast.2018.04.006.

[20] Center for International Earth Science Information Network (CIESIN), "Gridded Population of the World, Version 4 (GPWv4)," 2018. Accessed: 2020-06-20, 10.7927/H4PN93PB.